

Fidelity Charts and Stopping/Termination Criteria for Iterative Multiuser Detection

David P. Shepherd¹, Fredrik Brännström², Mark C. Reed³

¹National ICT Australia, Australian National University, Canberra, Australia, david.shepherd@anu.edu.au

²Dept. of Signals and Systems, Chalmers University of Technology, 412 58 Göteborg, Sweden, fredrikb@chalmers.se

³National ICT Australia, Australian National University, Canberra, Australia, mark.reed@nicta.com.au

Abstract

An iterative multiuser detection (IMUD) receiver is considered for a code-division multiple-access (CDMA) system with turbo codes. Fidelity is considered as a metric for convergence analysis and an approximation of fidelity as a function of variance of the log-likelihood ratios is introduced. Fidelity charts are compared with extrinsic information transfer (EXIT) charts as tools for convergence analysis and a close approximation of the relationship between fidelity and mutual information is proposed. We then use this function to approximate a closed form expression for the EXIT function of an interference canceller. Further, we propose a new stopping criterion for the turbo decoder and the IMUD receiver which achieves complexity saving of up to 50% over conventional designs.

1 Introduction

The 3rd Generation Partnership Project (3GPP) standard mobile communication system uses a combination of code-division multiple-access (CDMA) with turbo coding. Predicting the convergence behavior for even a moderate number of users is computationally demanding. Methods such as variance transfer and extrinsic information transfer (EXIT) analysis have been devised for describing the convergence behavior without the need to run large-scale simulations. The Fidelity chart was introduced in [1] and [2], and was shown in [3] to be similar to the EXIT chart in terms of accuracy.

We propose an approximation of fidelity as a function of variance which we define as the S function. While Fidelity and EXIT charts are essentially representing the same thing, there is no closed form representation of the relationship between fidelity and mutual information. We propose transfer function T expressing mutual information as a function of fidelity. We show that this function proves to be useful since a closed form solution exists for the variance transfer chart of an interference canceller (IC) [4].

In [5] Land and Hoeher proposed the use of mean reliability of the extrinsic log-likelihood ratios (LLRs) as a stopping criterion for turbo codes. We extend the work in [5] and propose a variant on stopping criteria for the iterative multiuser detection (IMUD) receiver and turbo decoder (TD) based on mean reliability.

2 System Description

The IMUD receiver consists of an IC and a TD as shown in Fig. 1 and was first described for convolutional codes in [4]. The turbo code is 3GPP compliant

and consists of symmetric parallel concatenated 8-state, rate 1/2 convolutional codes with generator polynomial $(G_r, G) = (015, 013)$. The trellis is terminated in the encoders and the overall code rate is $R = 1/3$ (no puncturing) and information block lengths range from 1296 up to 3856 bits [6]. We use an additive white Gaussian noise (AWGN) channel. The IC takes channel values Y and *a priori* input a_{IC} (from each of the K users) and outputs extrinsic information (on the coded bits for each user) E_{IC} which is de-interleaved and becomes the *a priori* input A_{TD} to the TD. On the first iteration of the receiver the *a priori* input to the IC is zero. The TD outputs extrinsic information (on the coded bits) E_{TD} and *a posteriori* output (on the information bits) D_{TD} . E_{TD} is interleaved and converted to soft bits $a_{IC} = \tanh(E_{TD}/2)$ which becomes the *a priori* input a_{IC} to the IC. Hard decisions are made on D_{TD} . Note that Fig. 1 shows the receiver for a single user. In reality there are K TDs, which feed their extrinsic output LLRs back to the single IC.

3 Fidelity and Mutual Information

Define the LLRs λ and the soft bits \hat{x} as

$$\lambda \triangleq \ln \left(\frac{p(\lambda|x=+1)}{p(\lambda|x=-1)} \right) \in \mathbb{R} \quad (1)$$

$$\hat{x} \triangleq \tanh \left(\frac{\lambda}{2} \right) = \frac{e^\lambda - 1}{e^\lambda + 1} \in [-1, +1] \quad (2)$$

where $x \in \{+1, -1\}$ can be either equiprobable information bits or coded bits. Due to the definition of the λ in (1), the conditional probability density functions

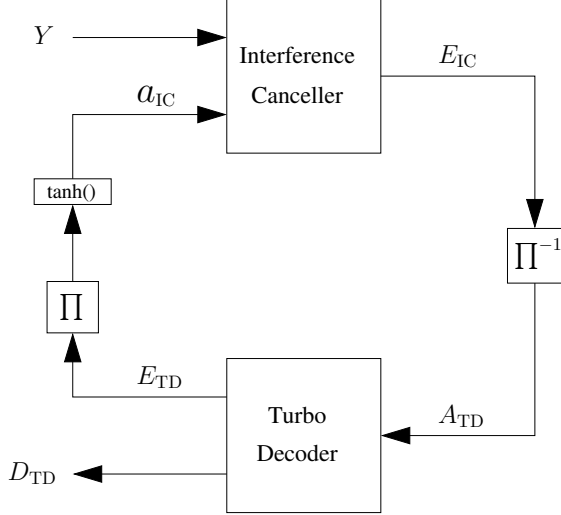


Fig. 1. IMUD receiver with IC and TD.

(PDFs) of λ have the following relationship [2]

$$p^+(\lambda) \triangleq p(\lambda|x = +1) = e^{+\lambda}p(\lambda|x = -1) \quad (3)$$

$$p^-(\lambda) \triangleq p(\lambda|x = -1) = e^{-\lambda}p^+(\lambda). \quad (4)$$

Hence, assuming equiprobable data, i.e. $x \in \{+1, -1\}$ the PDF of λ is

$$p(\lambda) = \frac{1}{2} (p^+(\lambda) + p^-(\lambda)) = \frac{1 + e^{-\lambda}}{2} p^+(\lambda). \quad (5)$$

Fidelity was first introduced in [1] and [2] as $E\{x\hat{x}\} = E\{x \tanh(\frac{\lambda}{2})\}$, where $E\{\cdot\}$ denotes expectation and λ the *a priori* (A) or extrinsic (E) LLRs for input and output fidelity respectively. We now show that fidelity can be estimated without knowledge of x . Using (2)–(5) we note that

$$\begin{aligned} E\{x\hat{x}\} &= \frac{1}{2} \int_{-\infty}^{+\infty} \hat{x} p^+(\lambda) d\lambda - \frac{1}{2} \int_{-\infty}^{+\infty} \hat{x} p^-(\lambda) d\lambda \\ &= \int_{-\infty}^{+\infty} \frac{\hat{x}(1 - e^{-\lambda})}{2} p^+(\lambda) d\lambda \\ &= \int_{-\infty}^{+\infty} \left(\frac{1 + e^{-\lambda}}{2} - \frac{2}{1 + e^{\lambda}} \right) p^+(\lambda) d\lambda \end{aligned} \quad (6)$$

and

$$\begin{aligned} E\{\hat{x}^2\} &= \frac{1}{2} \int_{-\infty}^{+\infty} \hat{x}^2 p^+(\lambda) d\lambda + \frac{1}{2} \int_{-\infty}^{+\infty} \hat{x}^2 p^-(\lambda) d\lambda \\ &= \int_{-\infty}^{+\infty} \frac{\hat{x}^2(1 + e^{-\lambda})}{2} p^+(\lambda) d\lambda \end{aligned} \quad (7)$$

Identifying that (7) and (2) can be rewritten as (6), we conclude that

$$M \triangleq E\{\hat{x}^2\} = E\left\{ \tanh^2\left(\frac{\lambda}{2}\right) \right\} \quad (8)$$

is equivalent to $E\{x \tanh(\frac{\lambda}{2})\}$. Hereafter, we will use M in (8) as the fidelity measure, since it can in contrast to $E\{x\hat{x}\}$ easily be estimated using a non-data-aided estimator based on L samples of the LLRs without knowledge of x , i.e.,

$$M \approx \frac{1}{L} \sum_{k=1}^L \tanh^2\left(\frac{\lambda(k)}{2}\right). \quad (9)$$

Define the variance σ_x^2 as the input/output variance from [4] and [7]

$$\sigma_x^2 \triangleq E\{(x - \hat{x})^2\} = 1 + E\{\hat{x}^2\} - 2E\{x\hat{x}\}. \quad (10)$$

Using (6)–(7), the following relationship is found

$$\sigma_x^2 = 1 - E\{x\hat{x}\} = 1 - E\{\hat{x}^2\} = 1 - M. \quad (11)$$

The mutual information between x and λ can be expressed as [8]

$$I = 1 - \int_{-\infty}^{+\infty} \log_2(1 + e^{-\lambda}) p^+(\lambda) d\lambda. \quad (12)$$

Assume λ has a mixed Gaussian distribution, i.e.,

$$\lambda = \frac{\sigma_\lambda^2}{2} x + n, \quad \text{where } n \in \mathcal{N}(0, \sigma_n^2). \quad (13)$$

Since the mutual information I in (12) cannot be expressed in closed form under the Gaussian assumption, close approximations were developed in [9] and [10] in form of the J function. The J function and its inverse defines the relationship between the mutual information I in (12) and the variance σ_λ^2 in (13), i.e.,

$$J(\sigma) \triangleq I(\sigma_\lambda = \sigma). \quad (14)$$

Using (5), the expression of the fidelity in (6) can be simplified to

$$M = 1 - \int_{-\infty}^{+\infty} \frac{2}{1 + e^{\lambda}} p^+(\lambda) d\lambda, \quad (15)$$

which is quite similar to the expression for the mutual information in (12). Therefore, we propose a function similar to J , the S function and its inverse, defining the relationship between σ_λ^2 and fidelity M . The S function is defined as

$$S(\sigma) \triangleq M(\sigma_\lambda = \sigma). \quad (16)$$

Since $S(\sigma)$ is monotonically increasing in σ_λ

$$\sigma_\lambda = S^{-1}(M) \quad (17)$$

where it is assumed that λ is Gaussian according to (13). Note also that using the relationship between the mutual information in (12) and the minimum mean-square error in (10) derived in [11], the following relationship between the J function and the S function is true

$$\frac{\partial J(\sigma)}{\partial \sigma} = \frac{\sigma - \sigma S(\sigma)}{\ln(16)}. \quad (18)$$

The S function has no closed form solution, but it can be closely approximated by

$$S(\sigma) \approx \left(1 - 2^{-H_1 \sigma^{2H_2}}\right)^{H_3}, \quad (19)$$

$$S^{-1}(M) \approx \left(-\frac{1}{H_1} \log_2\left(1 - M^{\frac{1}{H_3}}\right)\right)^{\frac{1}{2H_2}}, \quad (20)$$

where $H_1 = 0.4282$, $H_2 = 0.8130$ and $H_3 = 1.1699$ were obtained using the Nelder-Mead simplex method [12] to minimize the squared difference between the approximation and the actual function. The approximation of the S function in (19) has the same form as the approximation of the J function proposed in [10], i.e., using the constants $H_1 = 0.3073$, $H_2 = 0.8935$ and $H_3 = 1.1064$ in (19) give the approximation of the J function [10]. Fig. 2 shows the actual S and J functions along with their approximations, which are shown to be very close.

Since

$$\sigma_\lambda = J^{-1}(I) = S^{-1}(M), \quad (21)$$

we can express mutual information as a function of fidelity, this function is almost a straight line [7]. With the aim of deriving a close approximation to the exact relationship between mutual information and fidelity we propose a function $B(M)$ describing the difference between fidelity and mutual information

$$B(M) = M - I. \quad (22)$$

This function is shown in Fig. 3. Bounds on the B function were derived in [7]. We suggest the following approximation of $B(M)$

$$B(M) \approx 0.26(M - M^2), \quad (23)$$

where the constant 0.26 is chosen to approximately satisfy the actual difference when $M = 0.5$. The difference function (22) and the approximation in (23) are shown in Fig. 3, where we see the approximation is very close to the actual function. We then extend this to a transfer function between mutual information and fidelity

$$I = T(M) = J(S^{-1}(M)) \approx 0.74M + 0.26M^2, \quad (24)$$

$$M = T^{-1}(I) \approx \frac{-0.74}{0.52} + \sqrt{\left(\frac{0.74}{0.52}\right)^2 + \frac{I}{0.26}}, \quad (25)$$

which can be used to translate Fidelity charts into EXIT charts and vice versa. Due to the Gaussian assumption in the J and S functions, our proposed transfer function (24)–(25) also requires a Gaussian assumption on the distribution of λ .

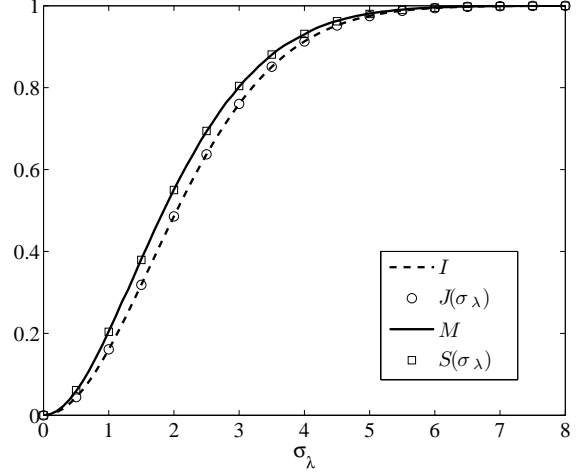


Fig. 2. Mutual information I (dashed line) and fidelity M (solid line) and their approximations, the J function (circles) and the S function (squares).

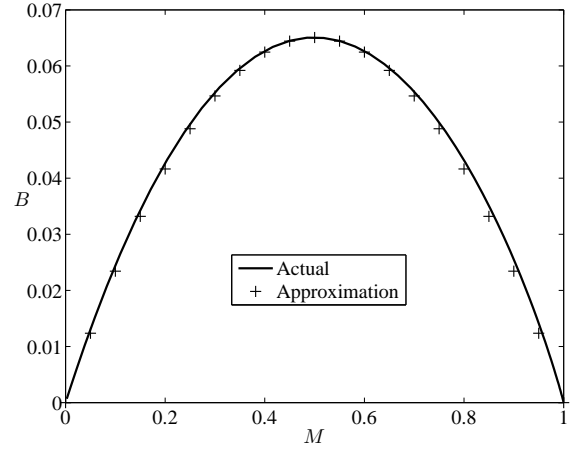


Fig. 3. Difference function $B(M) = M - I$, showing the actual function (solid line) and the approximation (crosses).

4 Convergence Analysis

The turbo receiver can be thought of as a three-dimensional decoder. This allows the decoding trajectory to be visualized in three dimensions. The transfer charts then become transfer surfaces and for the decoding to converge a tube must be open between the three surfaces. It is also possible to project this three-dimensional transfer chart onto a single two-dimensional chart as described in [10, 13]. However, instead of iterating between the decoders until convergence we limit the number of decoder activations to 6. That is, after each activation of the IC we run from 1 to 6 TD iterations before activating the IC again. The maximum number of TD iterations was determined arbitrarily through asymptotic performance analysis. The Fidelity and the EXIT charts for the 3GPP TD running 6 iterations are shown below in Fig. 4 as the solid unmarked curves. The transfer charts were found through Monte Carlo simulation of the TD

using an interleaver length of 3856 bits. The fidelity in Fig. 4(a) was calculated using (9) and the extrinsic mutual information in Fig. 4(b) was calculated using a non-data-aided method introduced in [13]

$$I_E^{\text{TD}} = 1 - 2\mathbb{E}\left\{\frac{\log_2(1 + e^{-E_{\text{TD}}})}{1 + e^{-E_{\text{TD}}}}\right\} \quad (26)$$

$$\approx 1 - \frac{2}{L} \sum_{k=1}^L \frac{\log_2(1 + e^{-E_{\text{TD}}(k)})}{1 + e^{-E_{\text{TD}}(k)}}. \quad (27)$$

We can also use (24)–(25) to translate EXIT charts to Fidelity charts and vice versa. The EXIT chart in Fig. 4(b) can be obtained using the Fidelity chart in Fig. 4(a) and (24) and the Fidelity chart in Fig. 4(a) can be obtained using the EXIT chart in Fig. 4(b) and (25).

A closed form solution exists for the variance transfer chart of an IC [4]

$$\frac{4}{\sigma_E^2} = \sigma_x^2 \left(\frac{K-1}{N}\right) + \sigma_n^2 \quad (28)$$

where $\sigma_E^2 = 4/\sigma_{\text{IC}}^2$ is the variance of the IC extrinsic output LLRs, σ_x^2 and σ_{IC}^2 are the variance of the input and output soft bits, respectively, as defined in (10), N is the spreading factor and $\sigma_n^2 = \frac{N_0}{2RE_b}$, where $R = 1/3$ is the code rate of the turbo code and E_b/N_0 is defined as the signal-to-noise ratio (SNR). The input variance σ_x^2 from [7] is equal to $\sigma_x^2 = 1 - M_A^{\text{IC}}$ using (11).

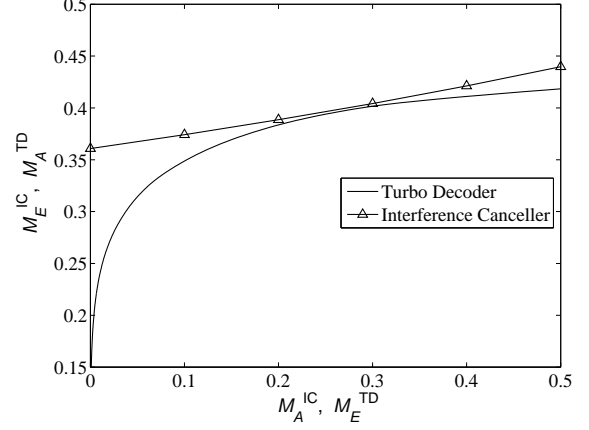
The fact that we have a closed-form solution for an IC variance transfer chart means that we can easily derive the transfer chart without the use of Monte Carlo simulation. The IC Fidelity chart can be derived using (28) to obtain σ_E and the S function to determine the corresponding value of M_E^{IC}

$$M_E^{\text{IC}} = S\left(\sqrt{\frac{4}{(1 - M_A^{\text{IC}})\frac{K-1}{N} + \frac{N_0}{2RE_b}}}\right). \quad (29)$$

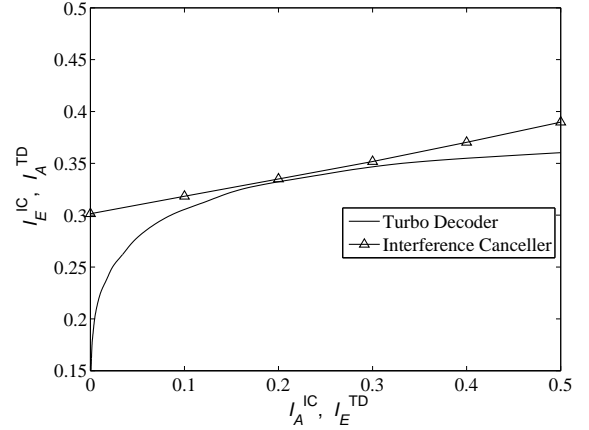
Derivation of the IC EXIT chart involves an extra step which is the translation of σ_x^2 to mutual information, that is

$$I_E^{\text{IC}} = J\left(\sqrt{\frac{4}{(1 - T^{-1}(I_A^{\text{IC}}))\frac{K-1}{N} + \frac{N_0}{2RE_b}}}\right). \quad (30)$$

Furthermore, both (29) and (30) require the usual Gaussian assumptions on the input LLRs (13), as for EXIT/Fidelity charts of component codes. In contrast to EXIT/Fidelity charts for component codes generated through Monte Carlo simulations, (29) and (30) also require that the output LLRs are Gaussian, which is in general true if K and N is not too small [4]. Refer to Fig. 4 for a convergence analysis for the IMUD receiver with a fully loaded system ($K = 20$ and $N = 20$). The fidelity and EXIT curve in Fig. 4(a) and Fig. 4(b) for the IC (marked with triangles) can be found using Monte Carlo simulations or by using (29) and (30), respectively. Note that both transfer charts predict a convergence threshold of $E_b/N_0 = 1.95$ dB.



(a) Fidelity Chart.



(b) EXIT Chart.

Fig. 4. Convergence analysis of the IMUD receiver at $E_b/N_0 = 1.95$ dB, $K = 20$ and $N = 20$.

A function to translate between EXIT charts and Fidelity charts is a useful tool since variance-based transfer charts (such as Fidelity charts) are useful for analysis of coded CDMA (among other) systems and EXIT charts are readily available in the literature for many forward-error correction decoders [8]. The transfer function in (24)–(25) can then be used to translate the transfer curves onto a common chart for analysis. Fidelity charts are convenient since, as shown in Fig. 1, we have soft bits with variance $\sigma_x^2 = 1 - \mathbb{E}\{a_{\text{IC}}^2\} = 1 - M_A^{\text{IC}}$ and extrinsic LLRs with variance σ_E^2 as IC input and output, respectively. Furthermore, online estimation of the IC extrinsic output fidelity is simple since (9) requires only a $M_E^{\text{IC}} = \mathbb{E}\{\tanh^2(E_{\text{IC}}/2)\}$ operation on the output extrinsic LLRs.

5 Stopping/Termination Criteria

Stopping and termination criteria are considered as a means of decreasing decoding complexity and delay. We define a stopping criteria as a detection of convergence and a termination criteria as determining when a target bit-error-rate (BER) has been reached.

We extend the work of Land and Hoeher [5] and use mean reliability as a stopping criteria in both the TD and the turbo receiver. Mean reliability is chosen since it is easier to calculate the mean of the LLRs than to estimate fidelity of mutual information. A decoder iteration is here referred to an iteration in the TD and a receiver iteration is the iteration between the IC and the TD. Mean reliability of the extrinsic (superscript e) output LLRs is defined as

$$\Gamma_i^e = E\{|E_i|\}, \quad (31)$$

where E_i is the extrinsic output of decoder $i = 1, 2$ in the TD. Decoding is stopped if Γ_1^e and Γ_2^e do not change in two subsequent iterations [5] of the TD.

We propose the use of the mean reliability of the extrinsic output of the TD, that is

$$\Gamma^e = E\{|E_{TD}|\}. \quad (32)$$

We also propose the use of mean reliability as a stopping criterion for the turbo receiver, where mean reliability is defined similar to (31), i.e., $\Gamma_{IC}^e = E\{|E_{IC}|\}$ and $\Gamma_{TD}^e = E\{|E_{TD}|\}$ are the mean reliability of the extrinsic output of the IC and TD in Fig. 1, respectively. Note that Γ^e is measured after each iteration in the TD, while Γ_{TD}^e is measured before each time the IC is activated. Decoding is stopped if there is no change in Γ_{IC}^e and Γ_{TD}^e over subsequent receiver iterations. We also use an LLR-based BER estimator [14]

$$\hat{P}_{b|\lambda} \triangleq E\left\{\frac{1}{1 + e^{|D_{TD}|}}\right\} \approx \frac{1}{L} \sum_{k=1}^L \frac{1}{1 + e^{|D_{TD}(k)|}} \quad (33)$$

as a receiver termination criterion, together with the above stopping criteria. In (33) $D_{TD}(k)$ denotes the k th information bit.

Assuming that the *a posteriori* output from the TD, D_{TD} in Fig. 1, is Gaussian as in (13), the BER can be predicted by the EXIT chart [8]. However, it can also be predicted based on the Fidelity chart as

$$\hat{P}_{b|M} \triangleq Q\left(\frac{S^{-1}(M_D^{TD})}{2}\right), \quad (34)$$

where $Q(\cdot)$ is the integral of the tail of a zero-mean Gaussian PDF with variance one and M_D^{TD} is the fidelity of D_{TD} .

We define the stopping/termination criteria as follows: Method 1 as our proposed new stopping criterion in the TD with LLR-based BER estimation termination using (33); Method 2 as our proposed new stopping criteria in both the TD and the turbo receiver with LLR-based BER estimation termination using (33); and the Land/Hoeher Method as the mean reliability stopping criterion from [5] in the TD with LLR-based BER estimation termination [14].

Fig. 5 shows a Fidelity chart for the IMUD receiver and illustrates the regions/points of activity of each of the stopping/termination criteria used. Only 1 and 6

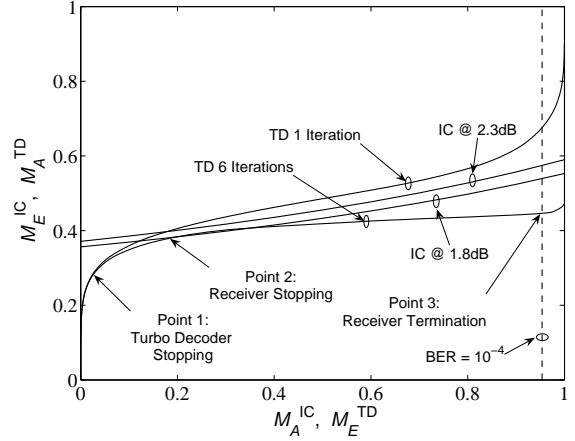


Fig. 5. Fidelity chart showing regions/points of activity of the stopping/termination criteria.

iterations of the TD are shown since the Fidelity chart of iteration 2 to 5 lie between these curves and are not necessary in this chart. The TD stopping criterion is active for decoder input fidelity of zero up to Point 1, that is for low fidelity input where there are no (significant) gains to be made from running more iterations of the decoder. Point 2 shows the convergence point of the system (in this case at $E_b/N_0 = 1.8$ dB), where the receiver stopping criterion is active since no further iterations of the receiver will improve performance once this point has been reached. The receiver termination criterion is active for decoder output fidelity greater than at Point 3. A fidelity $M_E^{TD} = 0.95$ of the bits fed to the IC corresponds to a BER of 10^{-4} . Note that this is the fidelity of the coded bits and corresponds to fidelity $M_D^{TD} = 0.9995$ of the information bits according to (34). Therefore, if the extrinsic output fidelity is greater than at Point 3 the BER estimator in (33) will be below 10^{-4} , which in this case is the target and therefore no further decoding is required.

The IMUD receiver was simulated for a loading of $K = 20$ with spreading factor $N = 20$. In each case a block length of 3856 bits was used with maximum of four iterations of the IMUD receiver and a target BER of 10^{-4} . Quantization of the mean reliability was considered and in each simulation Γ_i^e , Γ^e and Γ_{TD}^e were rounded to the nearest integer and Γ_{IC}^e was rounded to one decimal place, before comparison to previous iterations.

The simulation results of the stopping and termination criteria for Method 1 (diamonds) and Method 2 (dots) are shown in Fig. 6 and Fig. 7. For comparison we also show the performance of 4 iterations of the IMUD receiver running 6 iterations of the TD, i.e., no stopping or termination criteria activated (squares), the BER prediction based on Fidelity chart analysis (34) with no stopping or termination (crosses), and the Land/Hoeher Method (triangles). Our proposed new stopping criteria further reduce the complexity with

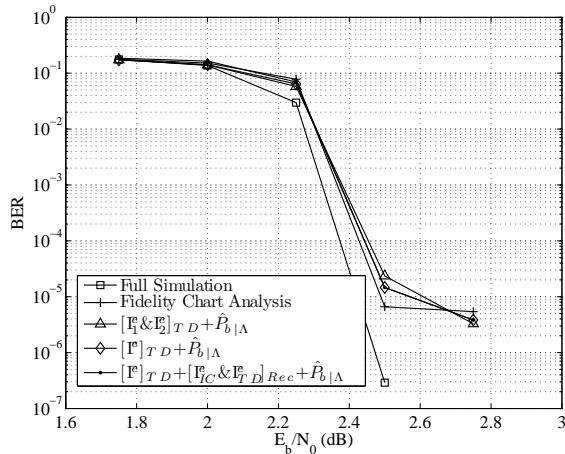


Fig. 6. BER performance analysis of the stopping/termination criteria.

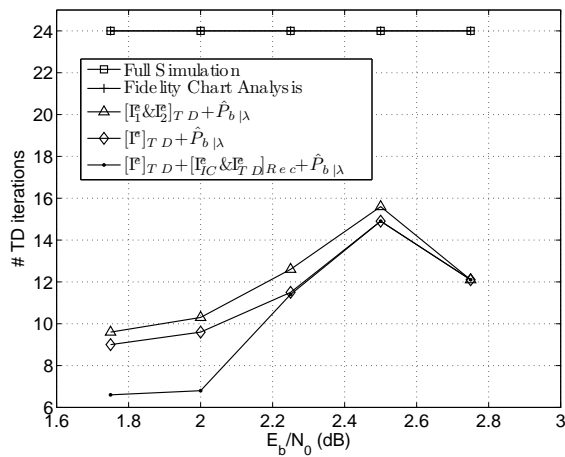


Fig. 7. Complexity (average total number of TD iterations) analysis of the stopping/termination criteria.

respect to [5], as shown in Fig. 7, without any significant degradation of BER performance. Typical cellular systems operate at frame error rates (FER) of 0.1 [6] which corresponds to a BER of approximately 3×10^{-3} or $E_b/N_0 = 2.35\text{dB}$ (for a block length of 3856 bits). At this operating point we save 1 iteration over [5] with a complexity saving of 50% over conventional designs. We assume the IC complexity is insignificant with respect to turbo decoder complexity.

We see that the stopping criterion in the receiver is only active for low SNR as shown by Point 2 in Fig. 5, and the termination criterion is only active for SNR greater than the turbo waterfall, as is evident from Fig. 5. Note that the waterfall in the simulation occurs at a slightly higher SNR than predicted in Section 4. This is due to the constraint we placed on the receiver of a maximum of 4 iterations and that we are only using a block length of 3856 bits, while EXIT/Fidelity charts analysis assumes infinite block lengths [8].

6 Conclusion

We introduced the S Function which gives a close approximation to the relationship between fidelity and variance. Furthermore, we extended the work in [7] and proposed a function $I = T(M)$ which gives a close approximation to the relationship between mutual information and fidelity. We applied these functions to a convergence analysis of a 3GPP compliant IMUD receiver utilizing an IC and a TD. We extended the work of Land and Hoeher and proposed new stopping/termination criteria to further reduce the decoding complexity and delay of the IMUD receiver.

References

- [1] K. Narayanan, "Effect of precoding on the convergence of turbo equalization for partial response channels," *IEEE Journal on Selected Areas in Communications*, vol. 19, pp. 686–698, April 2001.
- [2] J. Hagenauer, "The EXIT Chart - introduction to extrinsic information transfer in iterative processing," in *12th European Signal Processing Conference*, pp. 1541–1548, September 2004.
- [3] M. Tuchler, S. ten Brink, and J. Hagenauer, "Measures for tracing convergence of iterative decoding algorithms and channel coding," in *12th IEEE/ITG Conf. on Source*, (Berlin, Germany), pp. 53–60, Jan. 2002.
- [4] P. D. Alexander, A. J. Grant, and M. C. Reed, "Performance analysis of an iterative decoder for code-division multiple-access," *European Trans. on Telecom.*, vol. 9, pp. 419–426, Sep./Oct. 1998.
- [5] I. Land and P. A. Hoeher, "Using the mean reliability as a design and stopping criterion for turbo codes," in *2001 IEEE Information Theory Workshop*, pp. 27–29, September 2001.
- [6] "3GPP TS 25.104 V5.9.0; 3rd generation partnership project; technical specification group radio access network; base station (BS) radio transmission and reception (FDD) (release 5)," September 2004.
- [7] D. P. Shepherd, M. Ruan, Z. Shi, and M. C. Reed, "An analytical comparison of EXIT and variance transfer VT tools for iterative decoder analysis," in *Asilomar Conference on Signals, Systems and Computers*, 2005.
- [8] S. ten Brink, "Convergence behavior of iteratively decoded parallel concatenated codes," *IEEE Trans. Commun.*, vol. 49, pp. 1727–1737, Oct. 2001.
- [9] S. ten Brink, G. Kramer, and A. Ashikhmin, "Design of low-density parity-check codes for modulation and detection," *IEEE Trans. Info. Theory*, vol. 52, pp. 670–678, April 2004.
- [10] F. Brännström, L. K. Rasmussen, and A. J. Grant, "Convergence analysis and optimal scheduling for multiple concatenated codes," *IEEE Trans. Info. Theory*, vol. 51, pp. 3354–3364, September 2005.
- [11] D. Guo, S. Shamai, and S. Verdú, "Mutual information and MMSE in Gaussian channels," in *Proc. IEEE Int. Symp. Inform. Theory (ISIT '04)*, p. 349, June/July 2004.
- [12] J. A. Nelder and R. Mead, "A simplex method for function minimization," *The Computer Journal*, vol. 7, pp. 308–313, 1965.
- [13] F. Brännström, *Convergence Analysis and Design of Multiple Concatenated Codes*. PhD thesis, Chalmers University of Technology, Göteborg, Sweden, 2004.
- [14] P. Hoeher, I. Land, and U. Sorger, "Log-likelihood values and Monte Carlo simulation - some fundamental results," in *Int. Symp. on Turbo Codes and Rel. Topics*, pp. 43–46, September 2000.